

MATERIALS SCREENING METHODOLOGY FOR ADDITIVE MANUFACTURING IN BIOREACTOR TECHNOLOGY

J. Schorzmann¹, H. Gerstl¹, Z. Tan², L. Sprenger², H.-H. Lu³, S. Taumann¹, M. Wimmer¹, A.
R. Boccaccini³, S. Salehi-Müller², and F. Döpfer¹

¹Chair for Manufacturing and Remanufacturing Technology – University of Bayreuth, Bayreuth, Germany

²Chair for Biomaterials –University of Bayreuth, Bayreuth, Germany

³Institute of Biomaterials, Department of Materials Science and Engineering – University of Erlangen-Nuremberg, Erlangen, Germany

Abstract

Biofabrication is used to fabricate complex tissues/organs inspired by their native structures using additive manufacturing (AM) techniques and bio-inks (biopolymers enriched with living cells). Electroactive cells such as skeletal muscle function via electrical signals and therefore, their optimum *in vitro* functionality requires electrical conductivity and electrical stimulations. AM can be used to precisely fabricate a bioreactor for a dynamic culture of cells and bioengineered tissues and electrical stimulation of them. In this study, we focused on a material selection methodology for AM of bioreactors with selective electrical conductivity based on Reuter [1].

The important material requirements for bioreactors are biocompatibility, chemical stability, electrical conductivity, and the capability of being sterilized. However, there is no standardized procedure for selecting materials, that are appropriate for AM of bioreactors.

Our study comprises three phases which deductively narrowed down the material selection; these phases are the determination of material requirements, pre-selection, and fine selection of suitable materials. With the proposed method, a material selection for AM of functional bioreactors (consisting of bioreactor housing and integrated additively manufactured electrodes for electrical stimulation of the cells) could be efficiently made. For the bioreactor housing, two of the investigated materials, high-temperature polylactic acid (HTPLA) and polypropylene (PP) meet all requirements. The materials of the bioreactor electrodes could be narrowed down to polyethylene with copper particles (PE-Cu) and poly lactic acid with graphene nanoplates (PLA-GNP), where PE-Cu fulfilled all requirements besides the biocompatibility. PLA-GNP matches all requirements besides the high temperature resistance. For a final selection of the material for the bioreactor electrodes, further tests are required. However, this approach enabled to reduce the amount of biocompatibility testing from 16 different materials to only four (-75%), saving material, time, capacity and costs.

Keywords: Bioreactor Development, Material Screening Methodolgy, Additive Manufacturing, Material Extrusion With Thermal Reaction Bonding, Biofabrication, 3D-Bioprinting

Introduction

According to the US Department of Health & Human Services, there are approximately 120,000 patients only in the USA who are awaiting a life-saving organ donation. However, the existing donor pool stands at 5,200 as of June 2017 [2]. This significant disparity between the number of available organs and the demand for them presents a pervasive and formidable challenge to global medical care. In addition to the issue of limited availability, the high costs associated with transplantation and the occurrence of immune reactions to non-autologous organs often render the procedure infeasible for many patients [3].

Biofabrication (BF) is a technology that has garnered significant research attention in recent years, aiming to address these challenges. It encompasses an interdisciplinary approach, leveraging techniques from engineering sciences and biology, to create intricate and accurate replicas of organ and tissue structures *in vitro*. This is achieved through the utilization of bio-inks, which are biopolymers enriched with living cells. The process involves engineering of these bio-inks to fabricate complex and detailed organ and tissue structures. [2, 4, 5]

Following the BF process, the cells encapsulated in bio-ink are subsequently 3D printed and can be cultivated dynamically to undergo further maturation within a specialized system known as a bioreactor. This controlled environment provides the necessary conditions for the cells to proliferate and differentiate, leading to the formation of functional tissue [6]. The bioreactor serves as a dynamic system where various forms of stimulation, such as chemical, mechanical, electrical, and/or magnetic forces, are applied. These stimulations aim to replicate an *in vivo* growth environment for the cells. By mimicking the physiological cues and interactions found in living organisms, the bioreactor facilitates the development and maturation of the cells. This enables the cells to organize into functional tissue structures, that resemble the structures found in the body more closely [7]. The goal of the current study is to establish stimulation systems using two methods: directly (direct current flow in cells) or indirectly (via capacitor/coil, inducing electromagnetic fields) to investigate the role of external electrical stimuli within the context of BF. Consequently, it is necessary to fine-tune specific technical parameters such as material design (need for insulating material for bioreactor housing and electrically conductive material for electrodes), mass flow, and stimulation when creating a tissue-specific, individual bioreactor [6, 8]. However, the development of individualized bioreactors with conventional manufacturing methods (subtractive or formative manufacturing) is associated with problems such as the lack of possibilities for functional integration and limited geometrical freedom. This leads to the limited availability of individualized bioreactors ideally adapted to the respective tissue in clinical applications [7].

In the realm of researching alternative manufacturing technologies for bioreactors, additive manufacturing (AM) has gained significant attention from the scientific community. Due to the potential of AM (high geometrical freedom, functional integration, material and resource efficiency, multi-material capability), it can counteract the current problems in the manufacturing of bioreactors [7].

In the context of this paper, AM of an individual and functionalized bioreactor for the electrical stimulation of skeletal muscle cells is considered. Furthermore, AM possesses the capability to work with multiple materials, enabling the fabrication of complex bioreactors with diverse functionalities. This capability opens up new possibilities for the development of complex and functional living tissues within advanced bioreactors that can accurately replicate the *in vivo* conditions. The two components (bioreactor housing and electrodes) of the bioreactor can be manufactured simultaneously in one part composed of two different materials. However, an ideal AM process for the production of bioreactors is not yet identified [9]. This is primarily attributed to the high material demands associated with bioreactor manufacturing, making the selection of suitable materials a crucial factor in individual bioreactor development. The foremost requirement is biocompatibility, ensuring that the material does not harm the cells it encounters [10]. The bioreactor material should possess the capability of being sterilized through autoclaving and chemical treatment to eliminate potentially harmful microorganisms. Therefore, it is essential for the selected materials in the fabrication of the bioreactor to be resistant to substances such as ethanol or isopropanol, as well as maintain a high-temperature resistance exceeding 121 °C. Additionally, for the scope of this study, functional integration is needed in the form of an integrated electrode for transmitting electrical impulses to stimulate cultivated cells. Consequently, the bioreactor electrode material must also possess electrical

conductivity. However, there is still a scarcity of research findings regarding material selection in AM for bioreactors, necessitating further scientific investigations.

The primary objective of this paper is to select materials for each component (bioreactor housing and electrode) of the individualized and functionalized bioreactor, ensuring that their material properties closely align with the specified requirements (**Figure 1**). To achieve this goal, an application-specific material selection methodology will be developed, enabling the initial pre-selection of materials, and material characterization to evaluate the conformity of the material's property profile and the suitability of the pre-selected materials for the bioreactor components.

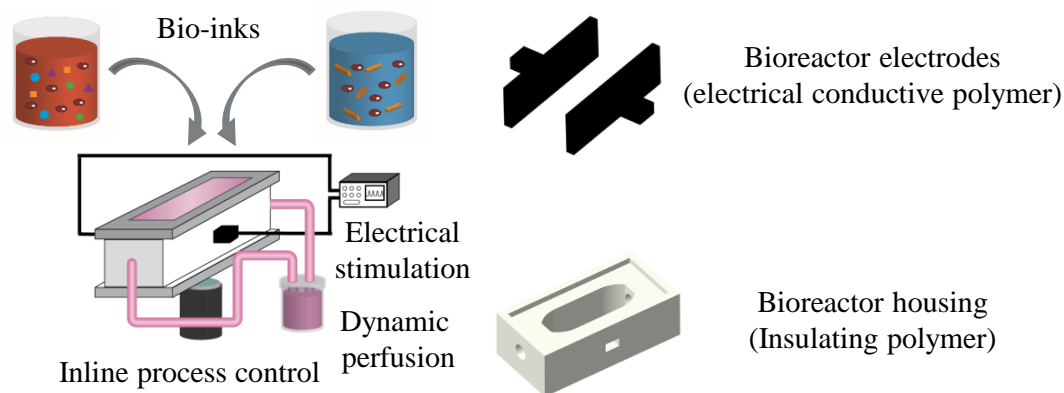


Figure 1 Example of a functionalized additive manufactured bioreactor concept

Methodology for material screening

The methodology for material selection in bioreactor development is founded upon Reuter's approach [1]. The material selection process, as per Reuter's methodology, is depicted in Figure 2 as a flowchart. This methodology is structured into three distinct phases: Phase I involves determining the material requirements, Phase II entails the pre-selection of suitable materials, and Phase III focuses on the fine selection and evaluation of materials [1].

This paper focuses primarily on Phases II and III, which involve an iterative process consisting of experimental verification and subsequent evaluation of material properties. The initial step involves a theoretical evaluation of materials using the evaluation scheme to assess their suitability for the bioreactor application. To validate the theoretical findings, material characterization is conducted to determine the property quantities. The corresponding property values are obtained through experimental tests. The statistical design of experiments is employed as the methodology to obtain reliable information about material properties while minimizing the number of required tests. In Phase II, the material's properties related to heat resistance, chemical resistance, and electrical conductivity, which are relatively easy to determine compared to biocompatibility, are evaluated. Subsequently, the materials providing the required properties in Phase II undergo tests for biocompatibility in Phase III, which forms the final material selection and concludes the entire material selection process.

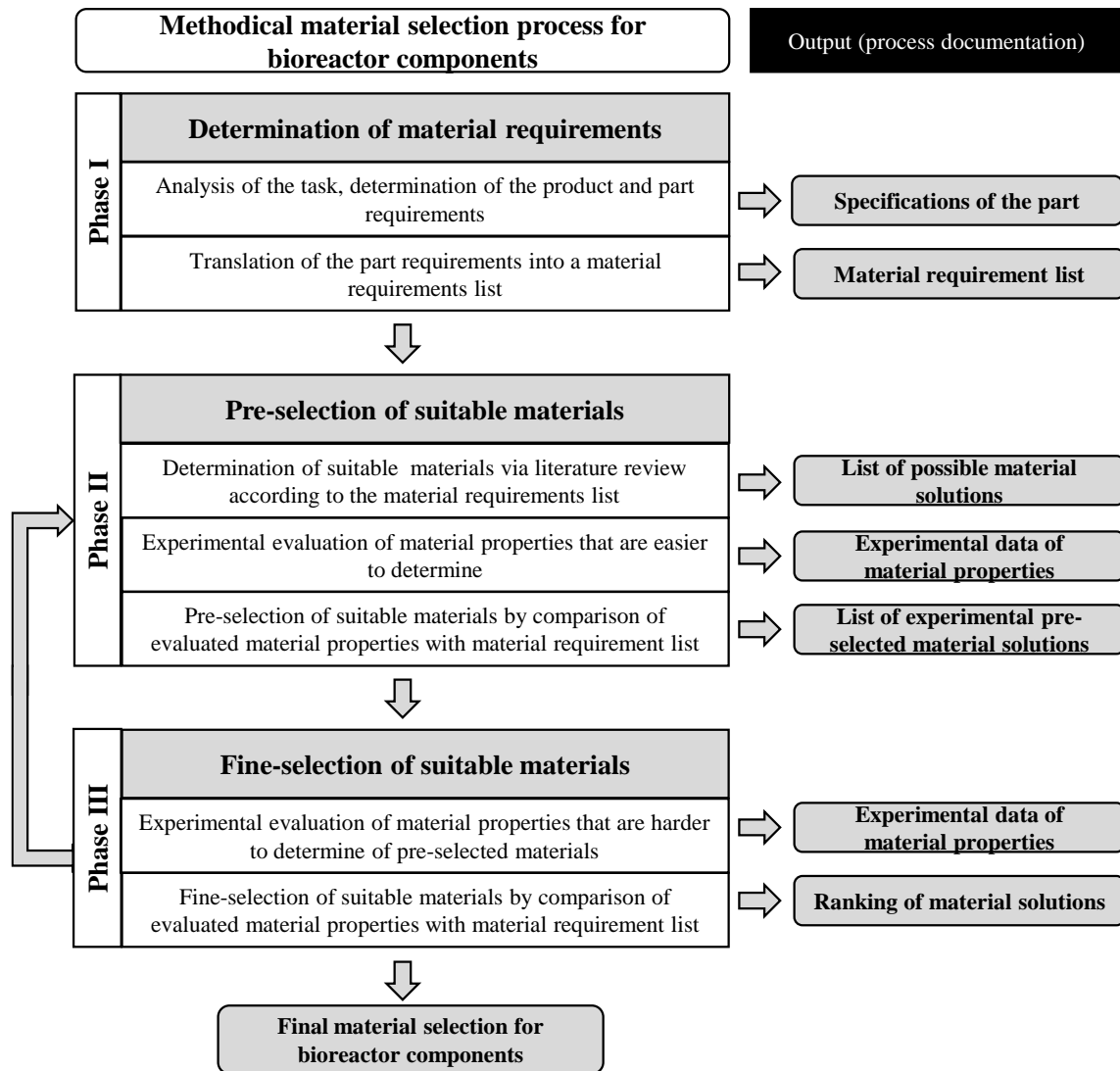


Figure 2 Methodological material selection process for bioreactor development

Phase I: Determination of material requirements

Phase I involves translating the product requirements into specific material requirements with defined properties. The outcome of this phase is a material requirement list that establishes the requirements profile for the material, forming the foundation of the search for an optimal material solution. The initial step in Phase I is to analyze the task and determine part requirements. This involves breaking down the bioreactor into its individual components and identifying the corresponding requirements for each component. [1]

In the BF field, bioreactors can play a vital role in promoting the maturation process of cells within bio-inks by applying physical stimuli. In this context, bioreactors function as dynamic systems capable of accurately replicating natural environmental conditions. For example, electrical stimulation can compensate the lack of innervation in the bioengineered tissues by giving impulses to the cells. This can be done by integrating a selectively electrically conductive material into the housing of the bioreactor as an electrode for generating an electric field and electrical stimulation of cells. [6, 7] Indeed, a multi-material (interchanging material within the layer) approach needs to be adopted for AM of the bioreactor. The first material used, should have insulating properties and serve as the housing of the bioreactor, providing a controlled environment for cultivating and proliferating the cells. The second material should be

electrically conductive and enable the generation of an electromagnetic field or a current flow in the bioreactor chamber for stimulating the cells. In addition to the functional requirements, the materials employed for manufacturing the bioreactor components must possess the essential characteristic of biocompatibility. This means that they should not release any substances that could harm the cells. Ensuring biocompatibility is crucial for maintaining a favorable environment for cell growth within the bioreactor.[8, 11, 12] Furthermore, the sterilization of the bioreactor via autoclavation and chemical treatment (ethanol or isopropanol) requires the chemical and thermal stability of the material. Following an overview of the part requirements in means of bioreactor development is listed:

- Biocompatibility
- Sterilization via autoclavation
- Sterilization by chemical treatment
- Stimulation of cells by an electromagnetic field or current

The target values are defined for each function and the part requirements are then converted into material requirements by means of a requirements analysis. For the determined material requirements property values are defined which describe the property profile of the material. Finally, a list of material requirements is drawn up in which quantitative target and limit values are assigned to the property values. Quantitative property values can be easily compared by assigning numerical values, e.g. for the melting temperature of a material. [1]

Phase II: Pre-selection of suitable materials

In Phase II of the material selection process, the objective is to identify materials that closely align with the defined material requirement profiles. This is achieved by selecting materials with the highest possible match in terms of their material property profiles, using the elaborated material requirement lists as a basis. The first step in Phase II involves conducting a literature review to define a list of materials that fit the considered material requirements from Phase I. Material requirements that are deemed suitable as search criteria for the material pre-selection are identified as evaluation criteria. Subsequently, the properties of the listed materials are experimentally evaluated to obtain reliable numerical values for these properties. In Phase II, the focus is primarily on assessing material properties that are relatively easy to determine. This approach helps to minimize the effort and costs associated with the experiments, particularly when obtaining data for biocompatibility.

During the selection process, evaluation criteria that incorporate quantitative property values play a crucial role. These criteria can be expressed numerically, facilitating direct comparisons between material property values. This numerical approach allows for a systematic assessment and ranking of materials based on their property profiles. Moreover, it is advantageous to identify evaluation criteria that have strict boundaries for property values. When certain property values fall out of the specified range, materials can be excluded from consideration. By deselecting materials that do not meet the required property values, the list of potential candidate solutions is narrowed down. This helps streamline the evaluation process, focusing the effort on a smaller subset of materials that are more likely to meet the desired criteria and requirements.[1]

Phase III: Fine selection and evaluation

Phase III of the Reuter material selection process involves refining the list of potentially suitable materials. In the first step, the materials are examined for their suitability with regard to evaluation criteria not yet considered in the pre-selection and further selected. Subsequently, the remaining materials are evaluated with regard to the correspondence of the property profiles

with the searched requirement profile by applying an evaluation procedure. The pre-selected materials from Phase II are evaluated in the case of the harder-to-determine material property, in this case the biocompatibility. Afterwards, each property value is compared as a deviation from the reference value. [1]

Additive manufacturing process

The process requirements established in Phase I include two main aspects: the ability to process polymers and the capability for multi-material printing. The need for multi-material capability arises from the requirement to simultaneously produce both the bioreactor housing and the electrode using different polymers - one non-conductive and the other conductive. A suitable AM process that fulfills this requirement is material extrusion with thermal reaction bonding (MEX-TRB), also called materialextrusion or fused deposition modeling, as depicted in Figure 3. Therefore, the subsequent process description and material selection will primarily focus on MEX-TRB as the chosen AM technique.

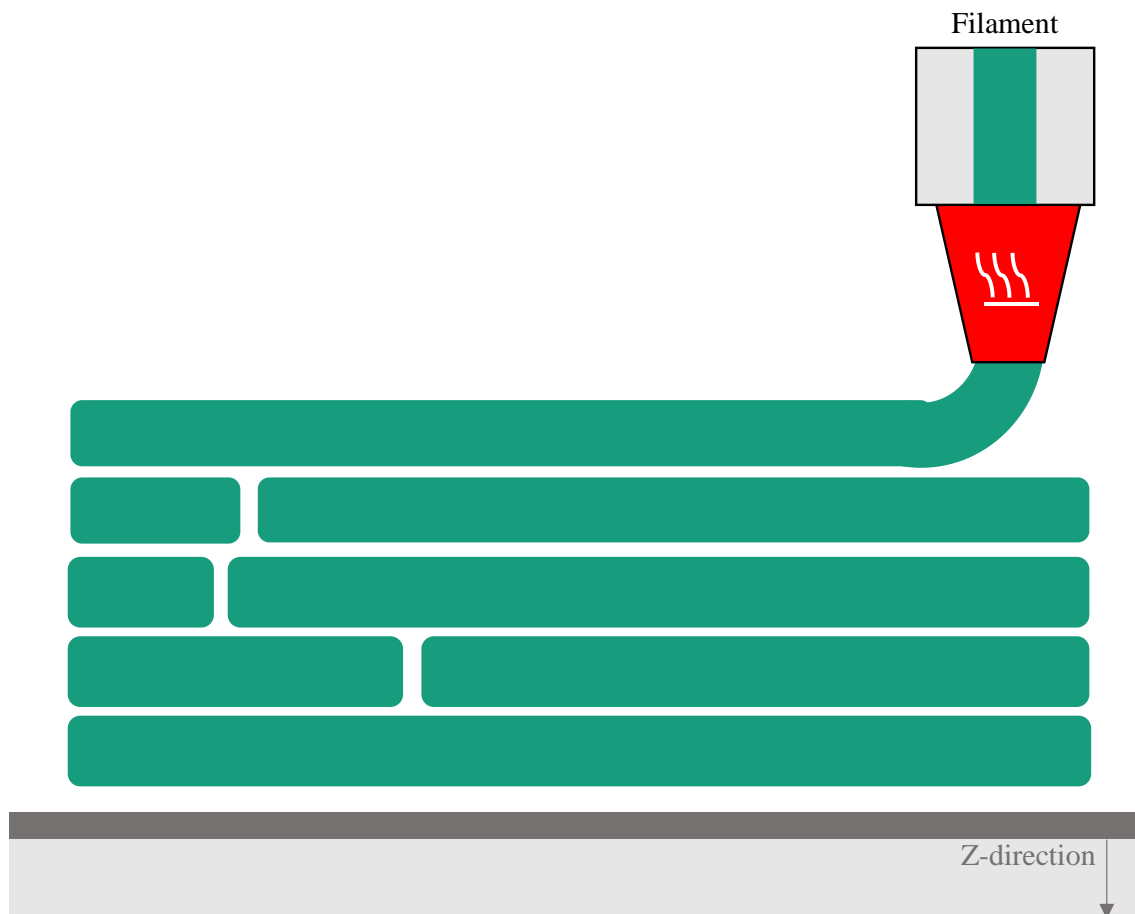


Figure 3 Procedure of additive manufacturing process material extrusion with thermal reaction bonding

Using the MEX-TRB process specification, the material, which is in the form of a thin filament, is melted by a heated nozzle and then applied in layers to a build plate [13, 14]. Thermoplastic polymers are used for processing because they can be melted and recrystallized any number of times without changing their material properties. For extrusion, the melted material is fed through the nozzle, which is attached to an extrusion print head [15]. The extrusion print head moves in the x-y plane according to previously defined coordinates and applies the molten material to the build plate. There, the material cools down and solidifies. After the completion

of a layer, the build platform is lowered in the negative z-direction by the respective layer thickness and the process is repeated [13, 15–17]. MEX-TRB has also configurations of AM machines with two extrusion printheads and two nozzles. In this case, one nozzle is primarily used for the extrusion of the base material, while the other is used e.g. for the generation of support structures for overhanging geometries or to produce functional multi-material parts, composed out of a base material and a second functional material [16]. In this paper, all standardized specimens to evaluate material properties by analytical methods were manufactured by MEX-TRB.

Description of standardized test methods and specimen

Electrical volume resistance

The electrical resistance of conductive polymers was measured based on the DIN EN ISO 3915, as one of the materials criteria in charge carrier conduction. The geometry of the specimens is defined as 10 mm width, 70 mm length, and 3 mm thickness. The allowed limit deviation with regard to uniformity is about $\pm 5\%$. [18]

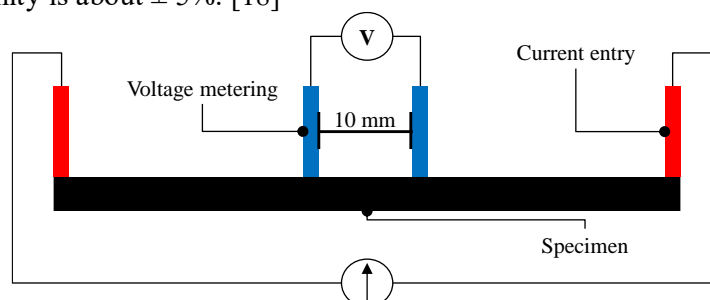


Figure 4 Four-point measurement according to DIN 3915

For the preparation of the measurements, the specimen surfaces are coated with four pieces of 5 mm wide strips of conductive silver paint. The experimental procedure follows the concept of the four-point method, in which two current and two measuring electrodes are used (see Figure 4). The current electrodes are attached to the outer contact points of the specimen. The two measuring electrodes are placed on the center of the two inner strips of conductive paint, with the required distance of 10 ± 0.2 mm between them [18]. At the start of the measurement, a stable direct current of magnitude I is passed between the two current electrodes placed at the ends of the material to be tested, and the potential drop ΔU between the measuring electrodes is measured with an electrometer [18]. The resulting resistance R is given by Equation 1.

$$R = \frac{\Delta U}{I} \quad \text{Equation 1}$$

For all specimens, a total of three individual measurements of R are carried out, with the measuring electrodes placed on the measuring strip with uniform distribution of the distances over the entire width. Subsequently, the arithmetic mean and the standard deviation are calculated for each specimen, and then, for interpretation and comparability of the results, the material-independent specific electrical resistance ρ is calculated according to Equation 2. The specimen cross-section A and the distance between the measuring electrodes d are also included in the calculation.

$$\rho = \frac{RA}{d} \quad \text{Equation 2}$$

Chemical resistance

The chemical resistance of the materials is measured based on DIN EN ISO 175 in contact with isopropanol and ethanol. In the first step, changes in the external appearance of the test specimens, such as swelling, degradation, the formation of cracks, or layer delamination, are determined by visual inspection and thus an initial estimate of the chemical resistance is made. [19] For the final evaluation, the dimensions of all specimens are then determined before and after contact with the chemicals (isopropanol and ethanol), and a deviation analysis is performed. The dimensions of the cube specimen are $10 \times 10 \times 10 \text{ mm}^3$. The dimensions are determined by a caliper gauge for measurements accurate to 0.1 mm. The sides of the specimens are marked and three measurements are taken at equal distances from each other in the x, y, and z directions. The approximate volume V_1 of each specimen is calculated from the average values for the lengths l_{1x} , l_{1y} , and l_{1z} . All specimens are then placed in a sealable beaker filled with the respective test liquid. The specimens must not touch each other and must be completely covered with the test liquid. The test setup is shown as an example in Figure 5. [19].

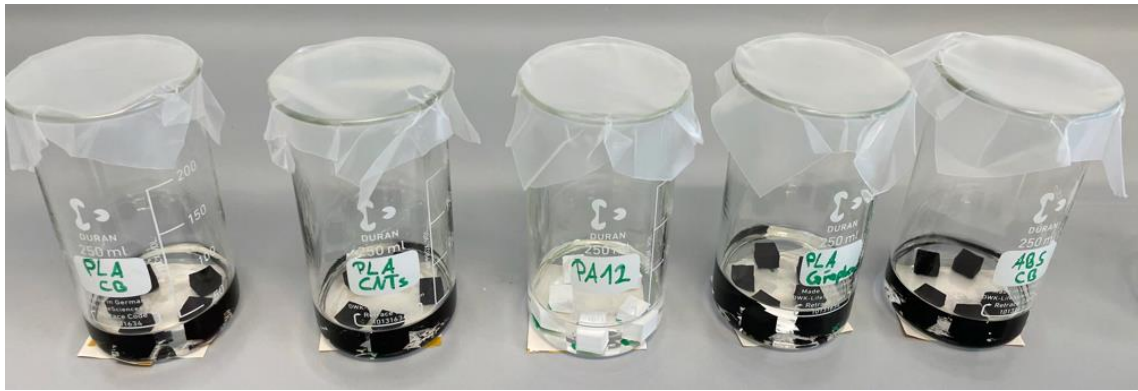


Figure 5 Test setup for testing chemical resistance (ethanol and isopropanol)

The test is performed for a defined duration of 24 h (short-term test) at a test temperature of 23 °C. After the test time has elapsed, the specimens are air-dried for further 24 hours. After drying, the dimensions of the specimens after testing are again determined, following the described procedure. The approximate volume V_2 of the respective specimen is calculated from the measured dimensions and from this the percentage swelling ratio Q is determined according to Equation 3. The lower the swelling ratio, the higher the material's resistance to the chemical.

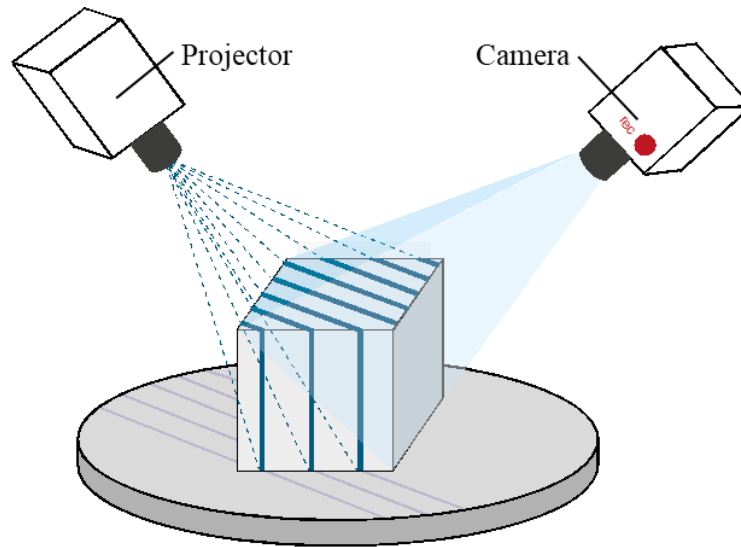
$$Q = \frac{V_2 - V_1}{V_1} * 100 \quad \text{Equation 3}$$

For the evaluation of the results, the Q values are averaged over all test specimens of one material and the standard deviations are calculated.

High-temperature resistance

Due to the absence of a standardized test setup for assessing the shape and dimensional accuracy requirements of the material under high-temperature conditions, the dimensions of the specimens can be freely chosen. However, the scanning method employed to measure the outer contours of the specimens imposes a limitation, as it can only detect specimens with an edge length exceeding 10 mm. Ultimately, a cubic specimen geometry with dimensions of $30 \times 30 \times 30 \text{ mm}^3$ is selected for the test. [20, 21] To ascertain the material suitability, the test specimens were immediately after production and prior to autoclaving optically imaged via a 3D scanner. The 3D scanner utilizes an optical non-contact measuring principle to capture the

surfaces of the test specimens and generate a digital model that accurately represents their shape and dimensions (refer to Figure 6) [22].



Measuring object on a rotary plate

Figure 6 3D scanning with optical non-contact measuring principle [22]

Subsequently, autoclaving is performed at 121 °C and 2.1 bar for a duration of 20 min. The evaluation of the specimens begins with a visual inspection, where any surface melting or significant deviations from the original cube-shaped geometry may indicate a lack of high-temperature resistance. Following the visual inspection, the geometry of all test specimens is re-captured using the 3D scanner. The GOM-Inspect software program is employed to compare the geometry of the specimens before and after autoclaving by superimposing their respective digital models.

This process allows a comparison of the geometric dimensions (before and after autoclaving). To provide a final assessment of the high-temperature resistance, the superimposed digital images of the specimens are sectioned three times along each coordinate axis plane of the x-y-z coordinate system (XY plane, XZ plane, and YZ plane). The largest deviation is recorded for each section (see Figure 7). The maximum deviation of the three sections in each coordinate axis plane is expressed for each specimen in terms of ΔXY_{\max} , ΔXZ_{\max} , and ΔYZ_{\max} . In addition, the average of the maximum deviation ΔXYZ_{\max} and standard deviation in each coordinate axis plane is formed over all specimens of a material.

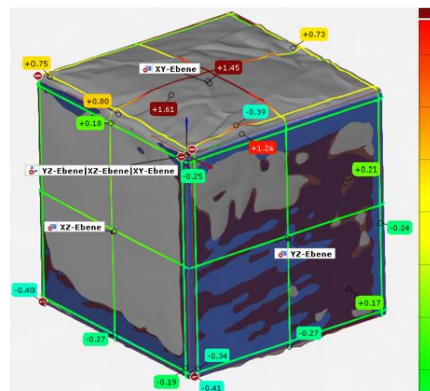


Figure 7 Digital images of the specimens sliced three times parallel to each coordinate axis plane of the x-y-z coordinate system (XY plane, XZ plane and YZ plane) to determine the maximum deviations.

Cytotoxicity

To test the cytocompatibility of the materials, the cytotoxicity test is determined based on DIN EN ISO 10993-5 and by measuring the metabolic activity using an Alamar Blue assay. First the test specimens were manufactured in the shape of square foil with an edge length of 30 mm and a thickness of 0.4 mm. To prepare sample extracts, 5-mm samples were cut using a biopsy punch, sterilized with ethanol and UV for 20 min and allowed to diffuse in C2C12 skeletal muscle cells culture medium by mixing continuously for 5 days. According to this standard, polyethylene was used as a negative and 1% Triton X-100 as a positive control. For the preparation of the samples, C2C12 cells were cultivated in culture medium with following composition: DMEM with 10% FBS, 0.4% glutamax, 1% penicillin-streptomycin and 2% 20mM HEPES solution. The cells were seeded into a 48-well plate with a cell density of 5000 cells/well. Upon 24 h of cell seeding, the culture medium was exchanged with 320 μ L of sample-diffused extract and positive control, and left for cell reaction in the incubator overnight. The samples were prepared with blanks (solely Alamar Blue), a negative control, and a positive control. After 24 h incubation of cells with extract, their methabolic activities were measured using amalar blue assay where the absorbance plate reader, with setting of 530 nm excitation wavelength and 600 nm emission wavelength was used. Each sample of this test is prepared and measured in triplicate and the standard deviation is calculated. According to the standards, a material meets the cytotoxicity requirements, if more than 70% of the cells are still viable after treatment over the specified test period [23].

Results

Phase I: Determination of material requirements

The part requirement of biocompatibility is translated into the material requirement of cytotoxicity, which refers to the ability of a substance to harm cells or tissues. Cytotoxicity is assessed by measuring the cell viability when in contact with the tested material. The desired target value for cell viability is set at over 70%, indicating that at least 70% of the cells in the test medium should survive.

For the bioreactor to generate an electromagnetic field within its chamber, electrodes made from an electrically conductive material are necessary. Therefore, one material requirement for the electrode material is electrical conductivity. The requirement for autoclavability and the subsequent sterilization through heat treatment leads to the material requirement of high-temperature resistance, which is evaluated by examining the shape and dimensional accuracy. The maximum dimensional deviation between the specimen before and after autoclaving should be limited to 0.28 mm. The part requirement of sterilization through chemical treatment can be translated into the material requirement of chemical resistance (to substances like ethanol or isopropanol). This is evaluated by examining the shape and dimensional accuracy and describing a swelling factor Q as an expression of volume changes.

Table 1 Material requirement list

Part requirement	Material requirement	Target value
Biocompatibility	Cytotoxicity	>70% cell viability
Sterilization via autoclavation	Shape and dimensional accuracy under high temperature	Deviation $\Delta XYZ_{\text{limit}} = 0.28$ mm by 121 °C and 1 bar 20 min
Sterilization via chemical treatment	Shape and dimensional accuracy against chemicals	Swelling factor $Q_{\text{limit}} = 2.5\%$ factor by 24 h
Electromagnetic field	Electrical volume resistance	<10 ³ Ω cm

Phase II: Pre-selection of suitable materials

The first step in Phase II is to generate a list of possible material solutions (see Table 2). First, a literature review must be done with a focus on finding sources that report proof of concepts of biocompatible polymers. At the same moment, these materials are screened in the context of processability and commercial availability within the defined AM technologies, in this case MEX-TRB.

Table 2 List of pre-selected materials from the literature review in general or bioreactor housing

Material	Processability with MEX-TRB and commercially available material	Literature review with proof of concept of biocompatibility
Acrylnitril-Butadiene-Styrol-Copolymer (ABS)	Yes [24, 25]	Yes [10, 26]
Polyethylenterephthalat (PET)	Yes [27, 28]	Yes [29]
Polycarbonate (PC)	Yes [13, 27]	Yes [30]
Poly lactide acid (PLA)	Yes [25, 28]	Yes [10, 31]
Polyoxymethylene (POM)	Yes [28, 32]	Yes [33]
Polypropylene (PP)	Yes [28, 32]	Yes [29]
Polyamide 12 (PA 12)	Yes [24, 34]	Yes [26, 34]
Polymethylmethacrylate (PMMA)	Yes [28]	Yes [35]
Polyetheretherketon (PEEK)	Yes [25, 28]	Yes [10, 30]
Thermoplastic polyurethane (TPU)	Yes [25, 28]	Yes [10, 35]
Polyethylene (PE)	Yes [28]	Yes [36]

Table 2 shows basically the materials for the bioreactor housing. The pre-selection of the materials for the electrodes was conducted by evaluating the used polymer matrix as biocompatible. To generate electrical conductivity in polymers, the polymer matrix has to be additivated with electrically conductive nanomaterials like carbon nanotubes, graphene nanoplates, and carbon black or copper particles. So, the pre-selected materials for the electrodes were chosen with a general biocompatible polymer matrix (see Table 3)

Table 3 List of pre-selected materials for bioreactor electrodes

Polymer matrix	Nanomaterial	Material manufacturer
PLA	Carbon black (CB)	Proto-Pasta
PLA	Carbon nanotubes (CNT)	Fiber Force
PLA	Graphene nanoplates (GNP)	Black Magic 3D
ABS	Carbon black (CB)	ezPrint
PE	Copper particles (Cu)	Multi3D

The next step in Phase II is to evaluate the materials pre-selected from the literature experimentally in terms of material properties that are easier and/or cheaper to determine. In the context of this paper, the materials are evaluated in Phase II in terms of electrical conductivity, chemical and high-temperature resistance. The biocompatibility will be evaluated in Phase III with the pre selected materials out of Phase II. The experimental data of electrical conductivity, chemical, and high-temperature resistance are shown from Figure 8 to Figure 11. The statistical analysis was conducted for the data of the chemical and high-temperature resistance with Shapiro-Wilk to determine normality, exclude outliers, and two-sample paired

t-test to define significance. The confidence interval was 95%, with $n = 5$ item numbers. The level of significance was set to $p \leq 0.05$. Considering clinical applications, the relative changes compared to the reference specimens were calculated. In this statistic, the significant difference was $Q_{\text{limit}} = \pm 2.5\%$ respectively $\Delta XYZ_{\text{limit}} = 0.28 \text{ mm}$ for one sterilization cycle.

Electrical conductivity

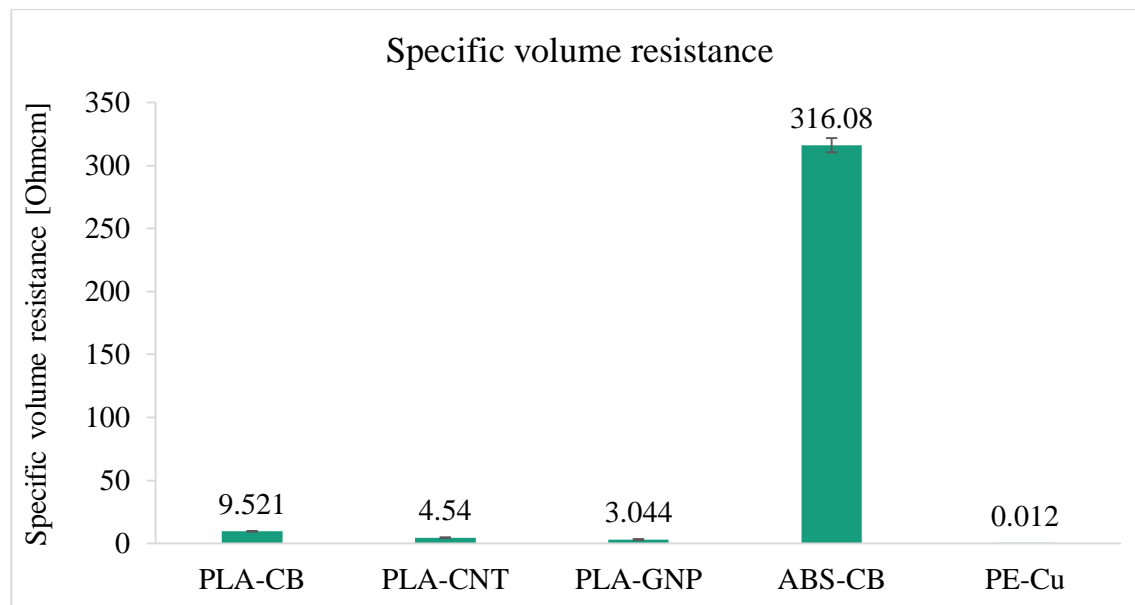


Figure 8 Results of specific volume resistance of electrically conductive materials for bioreactor electrodes

Analyzing the results of the pre-selected materials in means of specific volume resistance PE-Cu has the lowest value with $0.012 \pm 0.003 \text{ Ohmcm}$ and ABS-CB has the highest value with $316.08 \pm 5.644 \text{ Ohmcm}$. There between the materials PLA-CB ($9.521 \pm 0.244 \text{ Ohmcm}$), PLA-GNP ($3.044 \pm 0.464 \text{ Ohmcm}$), and PLA-CNT ($4.540 \pm 0.346 \text{ Ohmcm}$) were enqueued.

Chemical resistance

At the beginning of the analysis of the chemical resistance of materials to ethanol and isopropanol, a visual inspection is carried out on the test specimens. Based on this, an initial assessment of the material's resistance can be made by observing any visible changes in surface, volume, or material composition, such as swelling, delamination, or cracking. The materials, where the visual inspection of the test specimen revealed abnormalities, are shown in Table 4. After testing the chemical resistance of PA12 specimens against ethanol, a slight swelling is observed during the visual inspection. Additionally, significant layer delamination occurred in one of the specimens. However, no new abnormalities can be identified externally after testing with isopropanol. The PMMA specimens also exhibit slight swelling during the ethanol test. Additionally, there are minor vertical crack formations observed in relation to the applied layers. These effects are further intensified by the isopropanol test. However, after testing the chemical resistance to isopropanol and ethanol, a slight layer delamination is observed in one of the specimens of PLA-GNP. As for the PLA-CNT specimens, significant layer delamination occurred after the ethanol test, which is further intensified by the isopropanol test. The specimens, where no abnormalities were detected during the visual inspection, are presented in Table 5.

Table 4 Materials with optical abnormalities after chemical resistance test

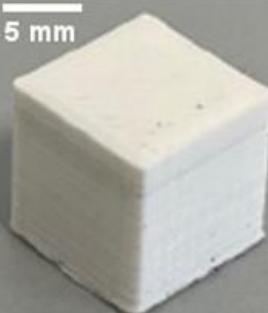





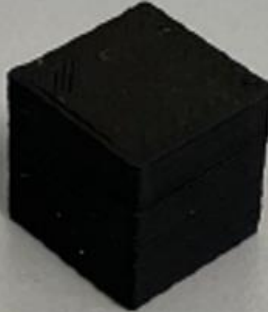

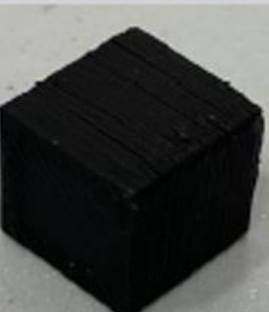
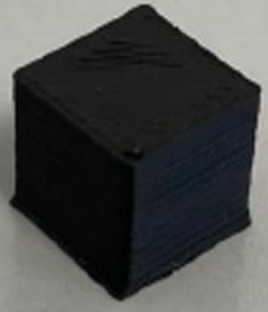
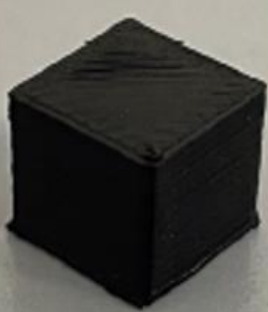
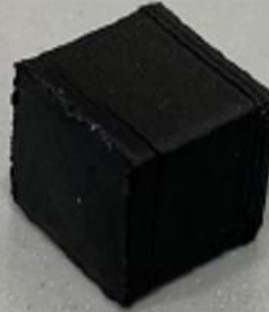
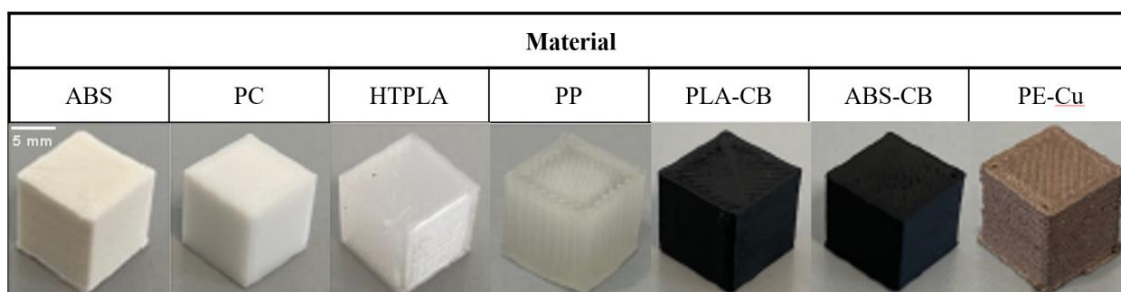
Material	Specimen after AM	Specimen exposition Ethanol	Specimen exposition Isopropanol
PA12	 <p>5 mm</p>		
PMMA			
PLA-CNT			
PLA-GNP			

Table 5 Materials without optical abnormalities after chemical resistance test



In the case of ABS, PC, PP, PLA-CB, PLA-GNP, and ABS-CB no significant changes in the t-test were observed. If the swelling factors are considered, no relative change has exceeded the limit value (ABS: $Q_{\text{ethanol}} = 0.065\%$, $Q_{\text{isopropanol}} = 0.026\%$; PC: $Q_{\text{ethanol}} = -0.053\%$, $Q_{\text{isopropanol}} = 0.093\%$; $Q_{\text{ethanol}} = -0.027\%$, $Q_{\text{isopropanol}} = -0.007\%$; PLA-CB: $Q_{\text{ethanol}} = 0.143\%$, $Q_{\text{isopropanol}} = -0.0865\%$; PLA-GNP: $Q_{\text{ethanol}} = 0.594\%$, $Q_{\text{isopropanol}} = -0.827\%$; ABS-CB: $Q_{\text{ethanol}} = 0.034\%$, $Q_{\text{isopropanol}} = -0.020\%$). Regarding the materials HTPLA, PMMA, and PA12 the evaluation of the t-test showed a significant rel. change in volume for chemical resistance against ethanol, but no significant change for chemical resistance against isopropanol. While the swelling factor values for the HTPLA ($Q_{\text{ethanol}} = -0.175\%$, $Q_{\text{isopropanol}} = -0.092\%$) and PMMA ($Q_{\text{ethanol}} = 0.789\%$, $Q_{\text{isopropanol}} = 0.532\%$) do not exceed the limit value, it can be stated for PA12 that the material is not resistant to ethanol ($Q_{\text{ethanol}} = 4.175\%$), but is resistant to isopropanol. ($Q_{\text{isopropanol}} = -0.978\%$). For PLA-CNT and PE-Cu the chemical resistance against ethanol and isopropanol showed significance on the basis of the t-test. But none of the swelling factors exceeded the limit value (PLA-CNT: $Q_{\text{ethanol}} = 0.603\%$, $Q_{\text{isopropanol}} = 0.95\%$; PE-Cu: $Q_{\text{ethanol}} = 0.067\%$, $Q_{\text{isopropanol}} = 0.237\%$) (see Figure 10, Figure 9 and Table 6).

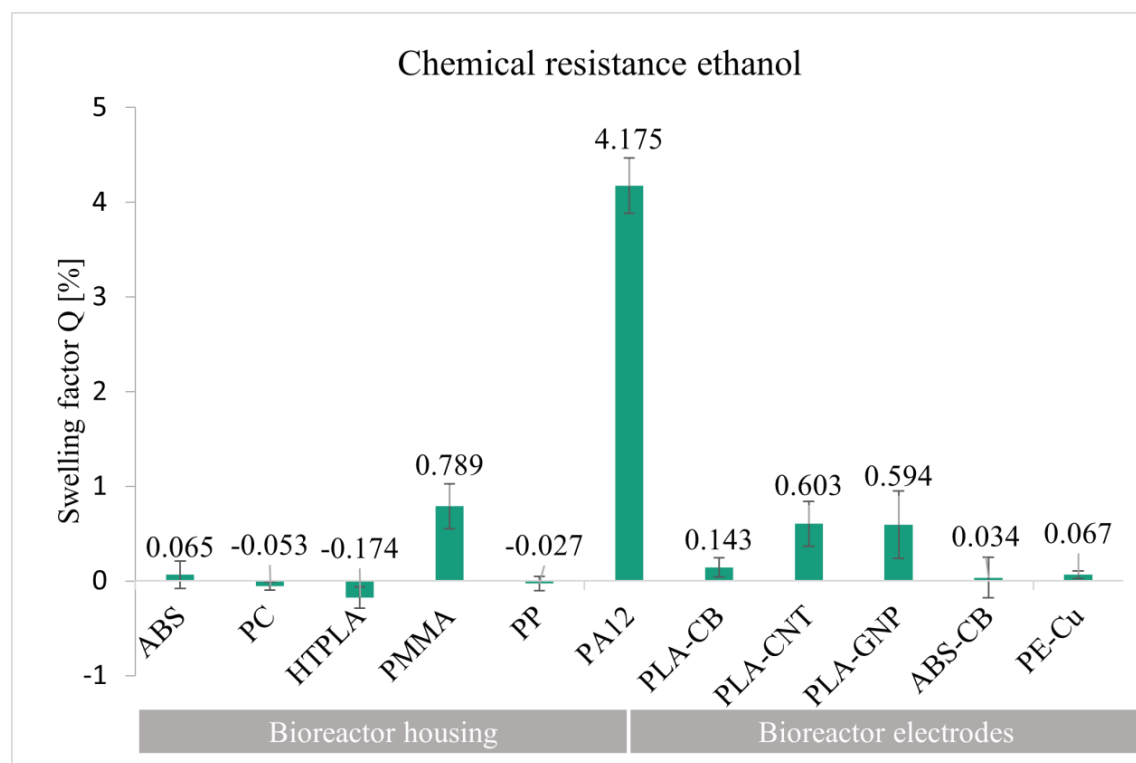


Figure 9 Results of chemical resistance against ethanol of pre-selected materials for bioreactor housing and electrodes

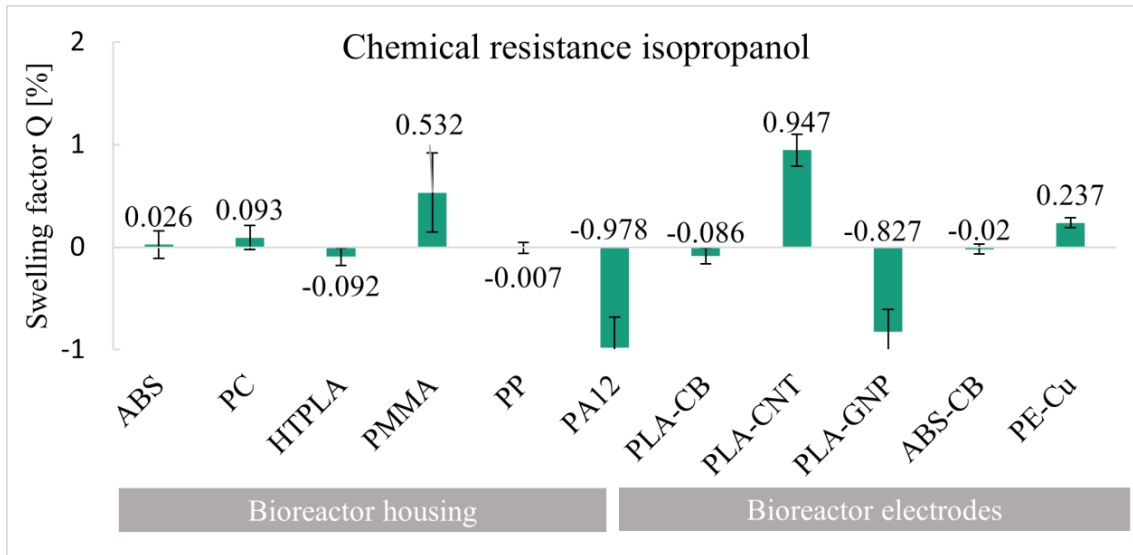


Figure 10 Results of chemical resistance against isopropanol of pre-selected materials for bioreactor housing and electrodes

Table 6 Statistical analysis of chemical resistance

Material	70% Ethanol				Isopropanol			
	AVG	SD	p (t-test)	Rel. Ch.	AVG	SD	p (t-test)	Rel. Ch.
Bioreactor housing	mm ³	mm ³		%	mm ³	mm ³		%
ABS	1067.66	16.69	0.445	0.065	1067.94	17.15	0.739	0.026
PC	1009.35	5.18	0.099	-0.053	1010.28	4.56	0.223	0.093
HTPLA	1073.58	9.14	0.05	-0.175	1072.44	8.19	0.124	-0.092
PMMA	1008.30	7.43	0.004	0.789	1013.65	8.23	0.065	0.532
PP	989.73	23.79	0.555	-0.027	989.67	24.30	0.844	-0.007
PA12	1089.28	12.63	0.001	4.175	1090.98	5.43	0.138	-0.978
Bioreactor electrodes								
PLA-CB	1057.57	5.66	0.063	0.143	1056.67	5.78	0.111	-0.0865
PLA-CNT	1037.17	7.84	0.011	0.603	1046.17	7.58	0.001	0.95
PLA-GNP	1012.01	7.37	0.074	0.594	1012.99	16.55	0.366	-0.827
ABS-CB	1026618,0	2.69	0.788	0.034	1026.41	3.39	0.509	-0.020
PE-Cu	969.34	2.32	0.001	0.067	970.65	17199,0	0.02	0.237







A significant change on t-test

High-temperature resistance

At the beginning of the high-temperature resistance evaluation of the materials, the specimens undergo a visual inspection, based on which an initial assessment of their resistance is made. Table 7 presents the materials, where the visual inspection of the specimens, after autoclaving, revealed abnormalities, indicating instability. Both ABS and ABS-CB exhibit slight surface melting and significant deformation of the originally cubic geometry in all specimens after autoclaving. As a result, the presence of high-temperature resistance can be excluded based on the visual inspection alone. Similar melting and deformation effects are observed in the PC specimens, albeit to a lesser extent compared to ABS and ABS-CB. No external abnormalities

are detected through the visual inspection of the HTPLA, PA12, PMMA, PP, PLA-CB, PLA-CNT, and PLA-GNP specimens.

Table 7 Materials with abnormalities after autoclavation

Material	<u>Specimen</u> after AM	Specimen after auto-clavation
PC		
ABS		
ABS-CB		

All tested materials have a significant change in shape and dimensional accuracy based on t-test analysis (see Table 8). The materials ABS, PC, PMMA, PA12, PLA-CB, PLA-CNT, PLA-GNP, and ABS-CB exceed the $\Delta XYZ_{\text{limit}}$ of 0.28 mm. These materials can be seen as not high-temperature resistant and cannot withstand the requirement of autoclavability (see Figure 11).

High temperature resistance



Figure 11 Results of high-temperature resistance of pre-selected materials for bioreactor housing and electrodes

HTPLA and PP as materials for bioreactor housing withstand the autoclaving process with shape and dimensional accuracy deviation before and after autoclaving of $\Delta XYZ = 0.277$ mm and $\Delta XYZ = 0.225$ mm, respectively. For bioreactor electrodes, PE-Cu is the only material that deceed the $\Delta XYZ_{\text{limit}}$ and can be classified as high temperature resistant as shown in Figure 11.

Table 8 Statistical analysis of high-temperature resistance

Material	Autoclavation 121 °C, 2.1 bar, 20 min			
	AVG	SD	p (t-test)	Rel. Ch.
Bioreactor housing	mm³	mm³		mm
ABS	31.4	0.320	0.017	1.403
PC	30.88	0.007	0.001	0.088
HTPLA	30.28	0.020	0.002	0.278
PMMA	30.50	0.120	0.020	0.499
PP	30.22	0.007	0.001	0.230
PA12	30.31	0.030	0.003	0.311
Bioreactor electrodes				
PLA-CB	30.61	0.014	0.001	0.612
PLA-CNT	30.76	0.059	0.002	0.764
PLA-GNP	30.85	0.086	0.003	0.851
ABS-CB	31.64	0.358	0.016	1.640
PE-Cu	30.17	0.025	0.008	0.167

A significant change in the t-test

In Table 9 the results of the material analysis are summarized and pre-selected to reduce the number of materials for the fine selection conducting the evaluation of biocompatibility. For bioreactor housing HTPLA and PP and for bioreactor electrodes only PE-Cu fulfill all tested requirements. ABS, PC, PMMA, PLA-CB, PLA-CNT, PLA-GNP, and ABS-CB are chemically resistant against ethanol and isopropanol but not high-temperature resistant. PA12 fulfills only one requirement of chemical resistance against isopropanol. For bioreactor housing HTPLA and PP are selected for further investigation of biocompatibility in Phase III. For bioreactor electrodes, PE-Cu is the only material that fulfills all requirements. Besides, the assessment of the order for the biocompatibility test additionally considers the level of electrical conductivity. Because PE-Cu also has the highest electrical conductivity, this material is on the rank number one for further biocompatibility tests. In order to have a certain comparability, a second material is selected for the bioreactor electrodes. Since no other material meets all three material requirements, the material with the next better electrical conductivity after PE-Cu is selected. Therefore, PLA-GNP is selected for biocompatibility tests in Phase III.

Table 9 List of experimental pre-selected material solutions

Requirement Material	Chemical resistance ethanol	Chemical resistance isopropanol	High temperature resistance	Ranking electrical conductivity	Order for Bio- compatibility tests
Bioreactor housing					
ABS	✓	✓	✗	-	6th
PC	✓	✓	✗	-	5th
HTPLA	✓	✓	✓	-	2nd
PMMA	✓	✓	✗	-	4th
PP	✓	✓	✓	-	1st
PA12	✗	✓	✗	-	3rd
Bioreactor electrodes					
PLA-CB	✓	✓	✗	4th	4th
PLA-CNT	✓	✓	✗	3rd	3rd
PLA-GNP	✓	✓	✗	2nd	2nd
ABS-CB	✓	✓	✗	5th	5th
PE-Cu	✓	✓	✓	1st	1st

Phase III: Fine-selection of suitable materials

In Phase III, the pre-selected materials are further examined for their suitability by using evaluation criteria that were not considered in Phase II. Therefore, material properties, that are harder to determine are investigated for the pre-selected materials. In the case of bioreactor materials, biocompatibility belongs to these harder-to-determine material properties. The Alamar Blue assay uses a resazurin-based solution acting as an indicator of cell health by using the reducing power of living cells to quantitatively measure cell viability. The resazurin-based solution is non-toxic to the cells and is able to diffuse through the cell membrane. It is blue in color and virtually non-fluorescent. After entering the cell, resazurin is reduced to resorufin, which is a red and highly fluorescent compound.

Figure 12 shows the results of the Alamar Blue assay for the tested, pre-selected materials PP, HTPLA, PE-Cu, and PLA-GNP from Phase II. To ensure validity and reliability of the assay, a

positive (toxic impact on the cells) and negative control (no toxic impact on the cells) are included. According to DIN EN ISO 10993-5, the material shows no cytotoxicity if the cell viability remains over 70% after the specified test period.

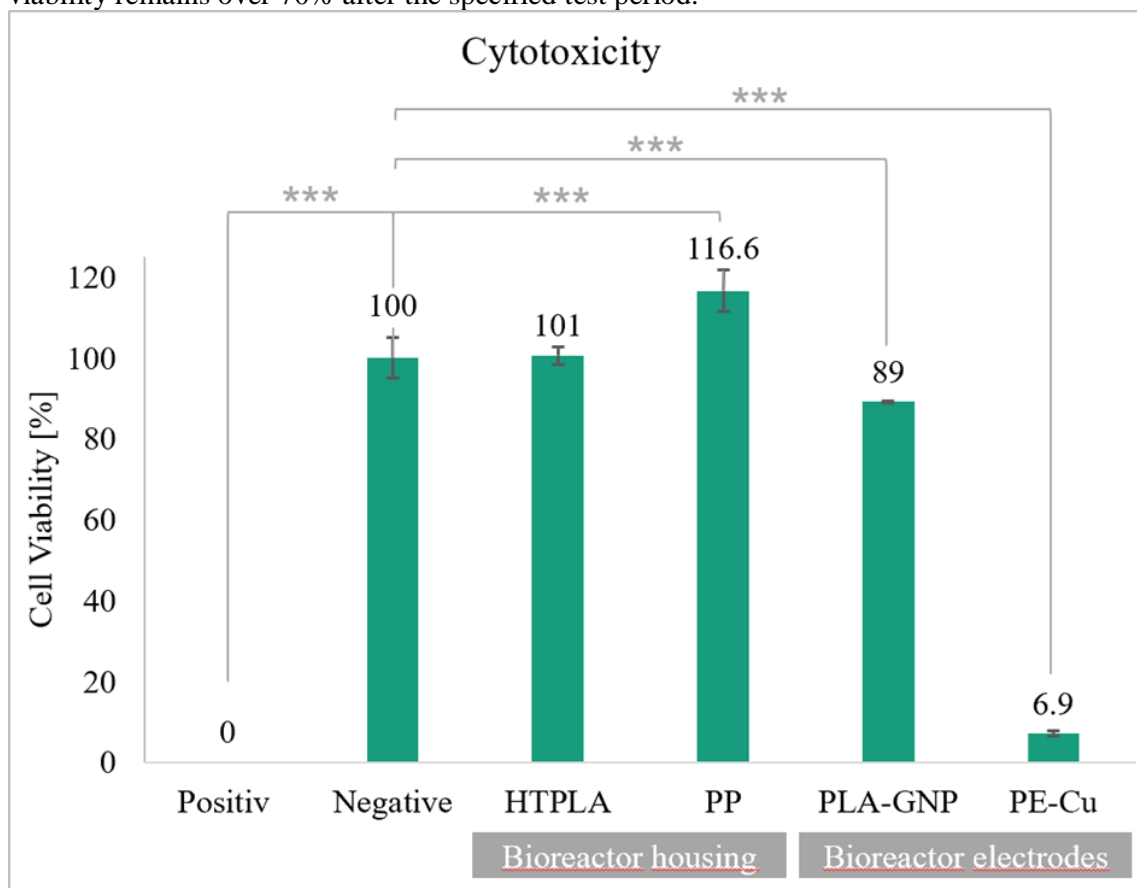


Figure 12 Results of cytotoxicity of pre-selected materials from Phase II normalized to negative control, * $p < 0.05$, ** $p < 0.01$, *** $p < 0.001$ statistical differences of means analysed via one-way ANOVA and Levene test

Both materials for the bioreactor housing, PP and HTPLA show no cytotoxicity to the cells after 24 hours of incubation with their extract and the cell viability of HTPLA remains the same and for PP even exceeds the cell viability of the negative control (100%). In contrast to that, the materials for the electrodes show a greater impact on the cells. PLA-GNP still leads to a cell viability of 89% but shows a significant difference to the negative control ($p < 0.001$). PE-Cu shows clear cytotoxicity with a cell viability of only 6.9%, which is only slightly less toxic than the positive control (0%). By respecting the cell viability limit of 70%, PP, HTPLA and PLA-GNP show biocompatibility, but due to the significant difference of PLA-GNP to the negative control, a long-term assay for PLA-GNP is considered necessary to ensure long-term biocompatibility. PE-Cu is highly cytotoxic and therefore does not fulfill the part requirement biocompatibility.

With the biocompatibility tests the material selection process is completed. Therefore, out of the list of pre-selected materials, PP and HTPLA are suitable for manufacturing the bioreactor housing and PLA-GNP for the electrodes, in terms of biocompatibility. But PLA-GNP did not fulfill the requirement of high temperature resistance in Phase II and was only selected for Phase III for comparative purposes. Subsequently, with the identified part requirements for the bioreactor electrodes, no material could be identified fulfilling all requirements. However, depending on the bioreactor design the electrodes do not have direct contact with the cells or the cell culture medium. Therefore, before excluding PE-Cu completely due to the lacking

biocompatibility, it can be checked in further tests, if the biocompatibility is met for test samples with the conductive material completely enclosed by the housing material. If these tests prove no cytotoxicity, the material requirements for the electrode material could be adapted, since they would not necessarily need to meet the requirement of biocompatibility anymore.

Conclusion

With this works, by applying the material selection process based on Reuter suitable materials for the bioreactor housing and for the electrodes could be detected. By applying this methodology, the number of possible materials from the pure literature research at the beginning of Phase II (eleven for the bioreactor housing and five for the electrodes) could be narrowed down to two materials for each bioreactor component, bioreactor housing (PP and HTPLA), and bioreactor electrodes (PE-Cu and PLA-GNP). In Phase III the properties that are harder to determine are investigated, in this case, the biocompatibility was tested. After Phase III both selected materials for the bioreactor housing were confirmed by the biocompatibility test and for the electrodes, PE-Cu could be identified as non-biocompatible. For the case that the electrodes do not have direct contact with the cells, or the cell culture medium, additional tests will be performed to analyze if embedding the material in the housing material may solve this issue. Nevertheless, the second selected material for the electrodes, PLA-GNP, showed good biocompatibility. But, it has to be considered, that PLA-GNP did not meet the deviation limit of 0.28 mm to fulfill the requirement of high temperature resistance (deviation ~ 0.8 mm) in Phase II and was only selected for Phase III for comparative reasons, since only PE-Cu fulfilled all requirements from Phase II. Therefore, it has to be checked whether the biocompatibility or high temperature resistance is more important for the bioreactor electrode material, to do a final selection. Generally, with this approach, the need for biocompatibility testing could be reduced from 16 different materials down to only four (-75%). Due to the narrowed down list of suitable materials, costs and effort of testing could be strongly reduced. For the future work the selected materials should be long-term tested with several autoclaving cycles (10 and 20 cycles) and longer exposure times to ethanol and isopropanol. Furthermore, in addition to shape and dimensional accuracy, the mechanical properties of the selected materials should also be investigated in short and long term experiments.

Acknowledgement

This research work was supported by the German Research foundation within the collaborative research center SFB TRR 225 Biofabrication.

References

- [1] Martin Reuter, *Methodik der Werkstoffauswahl: Der systematische Weg zum richtigen Material*, 3. Aufl. München: Carl Hanser Verlag, 2021.
- [2] S. Derakhshanfar, R. Mbeleck, K. Xu, X. Zhang, W. Zhong und M. Xing, „3D bioprinting for biomedical devices and tissue engineering: A review of recent trends and advances“ (eng), *Bioactive materials*, Jg. 3, Nr. 2, S. 144–156, 2018, doi: 10.1016/j.bioactmat.2017.11.008.
- [3] Y. Huang, X.-F. Zhang, G. Gao, T. Yonezawa und X. Cui, „3D bioprinting and the current applications in tissue engineering“ (eng), *Biotechnology journal*, Jg. 12, Nr. 8, 2017, doi: 10.1002/biot.201600734.
- [4] Mrunal S. Chapekar, „Tissue engineering: Challenges and opportunities“, *Biomed Mater Res (Appl Biomatter)*, Nr. 53, S. 617–620, 2000.
- [5] S. Ostrovidov *et al.*, „3D Bioprinting in Skeletal Muscle Tissue Engineering“ (eng), *Small (Weinheim an der Bergstrasse, Germany)*, Jg. 15, Nr. 24, e1805530, 2019, doi: 10.1002/smll.201805530.
- [6] D. Lim *et al.*, „Bioreactor design and validation for manufacturing strategies in tissue engineering“ (eng), *Bio-design and manufacturing*, Jg. 5, Nr. 1, S. 43–63, 2022, doi: 10.1007/s42242-021-00154-3.
- [7] L. Fu *et al.*, „The Application of Bioreactors for Cartilage Tissue Engineering: Advances, Limitations, and Future Perspectives“ (eng), *Stem cells international*, Jg. 2021, S. 6621806, 2021, doi: 10.1155/2021/6621806.
- [8] M. Gensler *et al.*, „3D printing of bioreactors in tissue engineering: A generalised approach“ (eng), *PloS one*, Jg. 15, Nr. 11, e0242615, 2020, doi: 10.1371/journal.pone.0242615.
- [9] B. M. Priyadarshini, V. Dikshit und Y. Zhang, „3D-printed Bioreactors for In Vitro Modeling and Analysis“ (eng), *International journal of bioprinting*, Jg. 6, Nr. 4, S. 267, 2020, doi: 10.18063/ijb.v6i4.267.
- [10] S. Vanaei, M. S. Parizi, F. Saleemizadehparizi und H. R. Vanaei, „An Overview on Materials and Techniques in 3D Bioprinting Toward Biomedical Application“, *Engineered Regeneration*, Jg. 2, S. 1–18, 2021, doi: 10.1016/j.engreg.2020.12.001.
- [11] G. Putame *et al.*, „Application of 3D Printing Technology for Design and Manufacturing of Customized Components for a Mechanical Stretching Bioreactor“ (eng), *Journal of healthcare engineering*, Jg. 2019, S. 3957931, 2019, doi: 10.1155/2019/3957931.
- [12] Spyridon Achinas, Jorn-Ids Heins und Janneke Krooneman and Gerrit Jan Willem Euverink, „Miniaturization and 3D Printing of Bioreactors:: A Technological Mini Review“, *Micromachines*, Nr. 853, S. 1–17, 2020, Art. no. 11. [Online]. Verfügbar unter: doi:10.3390/mi11090853
- [13] J. Ilg, *Systematische Eignungsanalyse Zum Einsatz Additiver Fertigungsverfahren: Anwendung Am Beispiel der Medizintechnik*. Wiesbaden: Gabler, 2019. [Online]. Verfügbar unter: <https://ebookcentral.proquest.com/lib/kxp/detail.action?docID=5622541>
- [14] Claudio Caviezel, Reinhard Grünwald, Simone Ehrenberg-Silies, Sonja Kind, Tobias Jetzke, Marc Bovenschulte, „Additive Fertigungsverfahren (3-D-Druck): Innovationsanalyse“, *TAB-Arbeitsbericht Nr. 175*, 2017.
- [15] M. Manoj Prabhakar, A. K. Saravanan, A. Haiter Lenin, I. Jerin leno, K. Mayandi und P. Sethu Ramalingam, „A short review on 3D printing methods, process parameters and materials“, *Materials Today: Proceedings*, Jg. 45, S. 6108–6114, 2021, doi: 10.1016/j.matpr.2020.10.225.

- [16] R. Lachmayer und R. B. Lippert, *Entwicklungsmethodik für die Additive Fertigung*. Berlin, Heidelberg: Springer Berlin Heidelberg, 2020.
- [17] M. Kumke, *Methodisches Konstruieren von additiv gefertigten Bauteilen*. Wiesbaden: Springer Fachmedien Wiesbaden, 2018.
- [18] *Kunststoffe: Messung des spezifischen elektrischen Widerstands von leitfähigen Kunststoffen*, 3915:2022-05, DIN Deutsches Institut für Normung e.V., Berlin, Mai, 2022.
- [19] *Kunststoffe: Prüfverfahren zur Bestimmung des Verhaltens gegen flüssige*, 175:2011-03, DIN Deutsches Institut für Normung e.V., Berlin, Mrz. 2011.
- [20] K. M. Fischer und A. P. Howell, „Reusability of autoclaved 3D printed polypropylene compared to a glass filled polypropylene composite“ (eng), *3D printing in medicine*, Jg. 7, Nr. 1, S. 20, 2021, doi: 10.1186/s41205-021-00111-x.
- [21] J. V. Chen, K. S. Tanaka, A. B. C. Dang und A. Dang, „Identifying a commercially-available 3D printing process that minimizes model distortion after annealing and autoclaving and the effect of steam sterilization on mechanical strength“ (eng), *3D printing in medicine*, Jg. 6, Nr. 1, S. 9, 2020, doi: 10.1186/s41205-020-00062-9.
- [22] C. Bay, T. Grotz, J. Kleylein-Feuerstein und J. Schorzmann, *Qualitätssicherung in der additiven Materialextrusion: Anwenderleitfaden für die Serienfertigung*. Stuttgart: Fraunhofer Verlag, 2022.
- [23] *Biologische Beurteilung von Medizinprodukten: Teil 5: Prüfungen auf In-vitro-Zytotoxizität*, 10993-5:2009, DIN Deutsches Institut für Normung e.V., Berlin, Okt. 2009.
- [24] S. Saleh Alghamdi, S. John, N. Roy Choudhury und N. K. Dutta, „Additive Manufacturing of Polymer Materials: Progress, Promise and Challenges“ (eng), *Polymers*, Jg. 13, Nr. 5, 2021, doi: 10.3390/polym13050753.
- [25] S. D. Nath und S. Nilufar, „An Overview of Additive Manufacturing of Polymers and Associated Composites“ (eng), *Polymers*, Jg. 12, Nr. 11, 2020, doi: 10.3390/polym12112719.
- [26] N. Poomathi *et al.*, „3D printing in tissue engineering: a state of the art review of technologies and biomaterials“, *RPJ*, Jg. 26, Nr. 7, S. 1313–1334, 2020, doi: 10.1108/RPJ-08-2018-0217.
- [27] Büro für Technikfolgen-Abschätzung beim Deutschen Bundestag, „Additive Fertigungsverfahren (3-D-Druck)“.
- [28] L. J. Tan, W. Zhu und K. Zhou, „Recent Progress on Polymer Materials for Additive Manufacturing“, *Adv. Funct. Mater.*, Jg. 30, Nr. 43, S. 2003062, 2020, doi: 10.1002/adfm.202003062.
- [29] M. F. Maitz, „Applications of synthetic polymers in clinical medicine“, *Biosurface and Biotribology*, Jg. 1, Nr. 3, S. 161–176, 2015, doi: 10.1016/j.bsbt.2015.08.002.
- [30] R. Pugliese, B. Beltrami, S. Regondi und C. Lunetta, „Polymeric biomaterials for 3D printing in medicine: An overview“, *Annals of 3D Printed Medicine*, Jg. 2, S. 100011, 2021, doi: 10.1016/j.stlm.2021.100011.
- [31] F. Calignano *et al.*, „Overview on Additive Manufacturing Technologies“, *Proc. IEEE*, Jg. 105, Nr. 4, S. 593–612, 2017, doi: 10.1109/JPROC.2016.2625098.
- [32] C. Feldmann und A. Pumpe, *3D-Druck – Verfahrensauswahl und Wirtschaftlichkeit*. Wiesbaden: Springer Fachmedien Wiesbaden, 2016.
- [33] K. J. Penick, L. A. Solchaga, J. A. Berilla und J. F. Welter, „Performance of polyoxymethylene plastic (POM) as a component of a tissue engineering bioreactor“ (eng), *Journal of biomedical materials research. Part A*, Jg. 75, Nr. 1, S. 168–174, 2005, doi: 10.1002/jbm.a.30351.

- [34] J. M. Jafferson und D. Chatterjee, „A review on polymeric materials in additive manufacturing“, *Materials Today: Proceedings*, Jg. 46, S. 1349–1365, 2021, doi: 10.1016/j.matpr.2021.02.485.
- [35] J. R. H. Sta Agueda *et al.*, „3D printing of biomedically relevant polymer materials and biocompatibility“ (eng), *MRS communications*, Jg. 11, Nr. 2, S. 197–212, 2021, doi: 10.1557/s43579-021-00038-8.
- [36] F. Puoci, *Advanced Polymers in Medicine*. Cham: Springer International Publishing, 2015.